Self-healing of Bessel-like beams with longitudinally dependent cone angles

I Litvin[1], L Burger[1,2], and A Forbes[1,3]

[1] CSIR National Laser Centre, P.O. Box 395, Pretoria 0001, South Africa
[2] Laser Research Institute, Physics Department, University of Stellenbosch, Stellenbosch 7602, South Africa
[3] School of Physics, University of the Witwatersrand, Private Bag 3, Johannesburg 2050, South Africa

E-mail: ilitvin@csir.co.za

June 2015 (preliminary version)

Abstract. Bessel beams have been extensively studied, but to date have been created over a finite region inside the laboratory. Recently Bessel-like beams with longitudinally dependent cone angles have been introduced allowing for a potentially infinite quasi non-diffracting propagation region. Here we show that such beams can self-heal. Moreover, in contrast to Bessel beams where the self-healing distance is constant, here the self-healing distance is dependent on where the obstruction is placed in the field, with the distance increasing as the Bessel-like beam propagates farther. We outline the theoretical concept for this self-healing and confirm it experimentally.

PACS numbers: (140.3295) Laser beam characterization; (140.3300) Laser beam shaping; (350.5500) Propagation; (050.1940) Diffraction

Keywords: Bessel-like beams, beam reconstruction, self-healing

Submitted to: *J. Opt.*

1. Introduction

Self-healing is a property that is usually associated with Bessel beams (BBs) [1–6], and describes the ability of the field to reform in amplitude after some distance beyond an obstruction. It is usually explained through a simple concept of rays: since the Bessel beam,

$$u(r) \propto J(k\theta r), \tag{1}$$

where $u(r)$ is the field of the Bessel beam, J is a Bessel function and $k = 2\pi/\lambda$ is the wave number of the incident light, may be seen as the interference of waves travelling on a cone of angle, θ, some waves may bypass the obstruction and hence interfere to create the original beam again [7].

Experimentally such self-healing was first demonstrated with zero-order BBs [8, 9], and later with BBs carrying orbital angular momentum [10]. More recently the concept of self-healing has been extended to other classes of optical fields, such as Airy beams [11], scaled propagation invariant beams [12] and rotating fields [13, 14], as well as to the angular domain [15] and beyond classical light to quantum states [7]. Self-healing of BBs has been a useful tool in a variety of applications ranging from communication [16], atmospheric studies [17, 18] microscopy [19–21] and optical trapping and tweezing [22–25]. Despite its many experimental demonstrations, it remains a topical field theoretically [26, 27].

A new class of BB was recently introduced where the intensity profile of the beam remains shape-invariant during propagation [28, 29]. This is in stark contrast to conventional BBs where the near-field is a Bessel function but the far field is an annular ring. In keeping with the literature we refer to such beams as Bessel-like beams (BLBs), which have a propagation-invariant Bessel-function intensity profile for a long propagation distance. These BLBs are engineered such that their cone angle is not constant but rather a function of propagation distance, $\theta(z)$. Based on this property we can assume that these beams will have self-healing properties similarly to Bessel beams but with a self-healing distance that is dependent on where the obstruction is placed in the field. Such behaviour has not been observed previously.

In this paper we study the self-healing properties of BLBs both theoretically and experimentally. We find that the self-reconstruction properties are similar to Bessel beams but that the self-reconstruction distance depends on the distance between the initial field (at the SLM plane) and the obstruction. This property is a result of the longitudinal dependence of the cone angle. This behaviour is a unique property of these beams in contrast with Bessel beams, where the self-reconstruction distance is constant.

2. Theoretical Approach

Consider the case where a BLB is created by a single phase-only element of the form

$$\varphi(r) = \exp[ik(ar^n + br^m)], \tag{2}$$

where k is the wave number of the incident light, and a, b, n and m are design parameters. If the clear aperture of the entrance optic is r_I, then the parameter set that gives rise to a BLB is given by [29]

$$b = -a\left(\frac{n}{m}\right) r_I^{n-m}. \tag{3}$$

Note that the phase terms in Eq. 2 can be viewed as optical aberrations, where the weights a and b necessarily obey the relationship in Eq. 3 in order to produce a long-range Bessel-like beam with reconstruction properties.

Now our BLB at any transverse plane can be written as the superposition of conical waves where the angle of arrival of the conical waves, $\theta(z)$, is identical and decreases with distance. The cone angles can be calculated from the stationary phase approximation to the diffraction equation, where rays from the source plane are mapped to new transverse positions at some distance z away. We provide the cone angles for some example hologram parameters in Table 1 (see appendix for details).

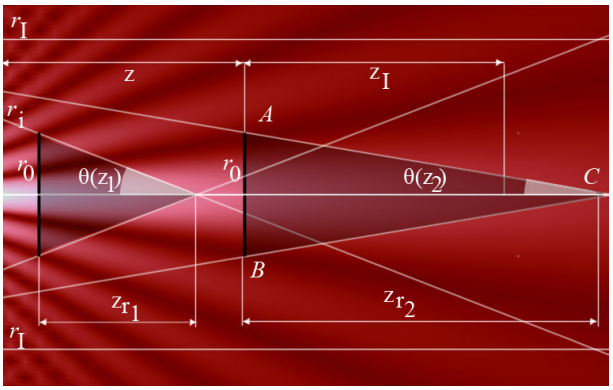

Figure 1. A longitudinal cross-section of the intensity distribution of a BLB illustrating the derivation of the self-reconstruction distance for BLBs. An obstruction with radius r_0 is located at z on the optical axis OC at position AB. Self-reconstruction occurs in the zone with length z_r.

To predict the reconstruction distance we make use of a simple geometric argument, but which is consistent with a full diffraction analysis. Consider

n=1; m=2	n=2; m=3	n=1; m=3
$\theta(z) = \frac{ar_I}{az - r_I}$	$\theta(z) = \frac{r_I}{12az^2}(1 + 10az \pm F(a,z))$ $F(a,z) = \sqrt{1 + 20az + 4a^2z^2}$	$\theta(z) = \frac{r_I}{6az^2}(r_I + 4az \pm G(a,z))$ $G(a,z) = \sqrt{(r_I)^2 + 8ar_Iz + 4a^2z^2}$

Table 1. The cone angle, $\theta(z)$, of BLBs for three example cases: $n = 1, m = 2$ (an axicon-lens doublet), $n = 2, m = 3$ (an aberrated lens) and $n = 1, m = 3$ (an aberrated axicon).

the scenario depicted in Fig. 1 where an obstruction of radius r_0 is placed in the path of the BLB at some distance z from the source. From simple trigonometric arguments we can see that the shadow distance, z_r, is given by the solution to

$$z_r = \frac{r_0}{\theta(z + z_r)}. \tag{4}$$

By way of example, consider the axicon-lens doublet in Table 1 ($n = 1, m = 2$) from which we find

$$\theta(z) = \frac{ar_I}{az - r_I}. \tag{5}$$

Substituting into Eq. 4 and solving for z_r we find

$$\begin{aligned} z_r &= \frac{r_0}{\theta(z + z_r)} \\ &= \frac{r_0[a(z + z_r) - r_I]}{ar_I} \end{aligned} \tag{6}$$

and thus

$$z_r(z) = \frac{r_0(az - r_I)}{a(r_I - r_0)}. \tag{7}$$

The same approach is followed for any parameter combination of the BLB, and example expressions are provided for various parameters sets in Table 2.

We note from Fig. 2 that the self-reconstruction distance depends on the distance between the initial plane and the obstruction. This behaviour is a unique property of BLBs in contrast to BBs where the self-reconstruction distance is constant. The representation of BLBs as the interference of two diverging conical-like waves helps to explain the nature of the self-reconstruction property which is similar to BBs [30]. For BBs the self-reconstruction distance is constant as a result of the constant cone angle, in contrast with BLBs where the self-reconstruction distance increases with distance as a result of the cone angle decreasing with distance, as shown in Fig. 1.

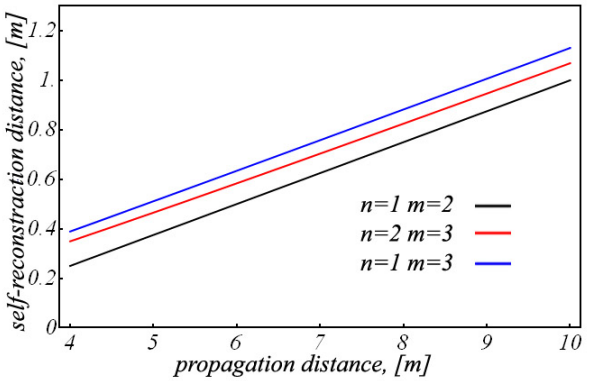

Figure 2. Dependence of self-reconstruction distance z_r (for certain values of n and m of the transformation system) on distance to obstruction z (see Fig. 1) for the following parameters of initial field and system: $w = 2$ mm, $r_0 = w/3$, $r_I = 3w$, $a = 3 \times 10^{-3}$; (black) $n = 1; m = 2$; (red) $n = 2, m = 3$; (blue) $n = 1, m = 3$.

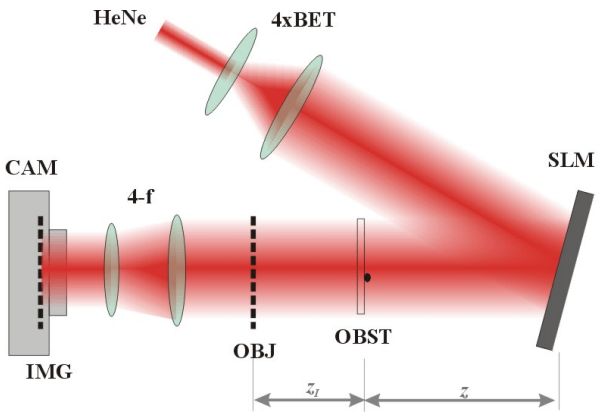

Figure 3. The experimental setup consists of an expanded HeNe beam reflected off the phase screen displayed on an SLM, creating a BLB with $n = 1, m = 2$. An obstruction OBST (either a bead or thin wire) was positioned at a distance of z from the phase screen. A 4-f imaging system transfers the object plane OBJ to the image plane IMG on the camera sensor CAM at several axial positions z_I.

3. Experimental results

For experimental verification a Gaussian beam from a HeNe laser was expanded by a 4× beam-expanding telescope (BET) to a beam radius $w = 1.7$ mm and reflected off a HoloEye PLUTO spatial light modulator (SLM). A phase screen was generated for a BLB with

n=1; m=2	n=2; m=3	n=1; m=3
$z_r(z) = \frac{r_0(az-r_1)}{a(r_I-r_0)}$	$z_r(z) = \frac{4ar_0z^2}{r_I-4ar_0z+2ar_Iz\pm r_I\sqrt{-\frac{8ar_0z}{r_I}+(1+2az)^2}}$	$z_r(z) = \frac{-2ar_0z^2}{2ar_0z\mp r_I^2\left(\pm1+\sqrt{1+\frac{4az}{r_I^2}(az-r_0)}\right)}$
	(+) for $a > 0$ and (-) for $a < 0$	(upper sign) for $a > 0$ (lower sign) for $a < 0$

Table 2. The self-reconstruction distance z_r for example values of n and m of the transformation system.

$n = 1, m = 2$ (equivalent to an axicon-lens doublet, and chosen to allow comparison with previous work, for example [31]) with $a = 0.05$ and $r_I = 2$ mm. An obstruction was placed at $z = 240$ mm from the SLM, and a series of transverse planes at z_I from the obstruction plane were imaged using a 4-f system onto an image plane coincident with the sensor of a Spiricon LBA-USB-L130 camera and recorded. The experimental setup is shown in Fig. 3.

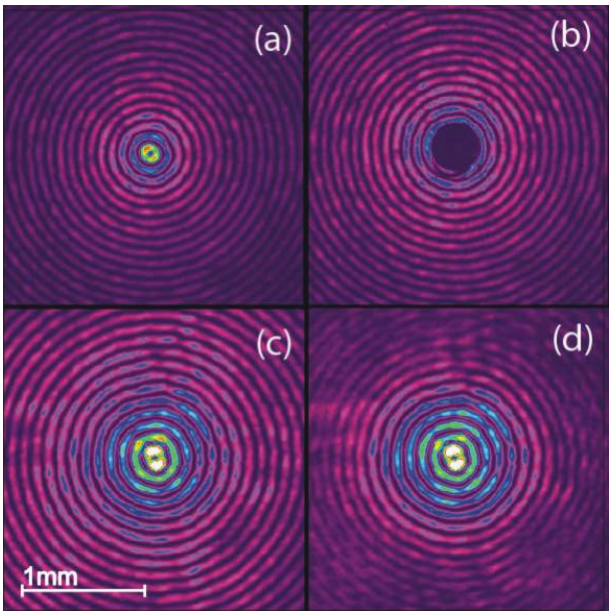

Figure 4. (a) Unobstructed BLB ($n = 1, m = 2, w = 1.7$ mm, $a = 0.05$) at the obstruction plane ($z_I = 0$), (b) BLB at the same plane but obstructed by a centred 400μm bead, (c) unobstructed BLB at $z_I = 110$ mm, and (d) obstructed BLB at $z_I = 110$ mm.

We first verified that reconstruction does indeed occur. The obstruction used consisted of a bead at the obstruction plane ($z_I = 0$) and centred on the BLB. We imaged this plane both without [see Fig. 4(a)] and with [see Fig. 4(b)] the bead. Notice the dark area at the centre of the beam in Fig. 4(b). We then moved our imaging system and camera a distance of $z_I = 110$ mm away, and imaged the beam at this point. Fig. 4(c) shows the unobstructed beam at $z_I = 110$ mm, and Fig. 4(d) shows the obstructed beam at the same plane. Notice that the ring structure of the beam has been completely reconstructed. We notice however that the intensity of the outer region of the obstructed beam (Fig. 4(d)) is lower than in the unobstructed beam (Fig. 4(c)).

In order to study how well other obstruction configurations would reconstruct we followed the method of the previous experiment, now using both a bead with diameter 400μm and a wire with diameter 180μm, in both centred and off-centred positions relative to the BLB, which was the same as generated previously, i.e. $n = 1, m = 2, w = 1.7$ mm, $a = 0.05$ and $r_I = 2$ mm. When in their off-centre positions the bead and the wire were respectively 839 μm and 526 μm from the centre of the BLB. For each obstruction configuration the beam was imaged and recorded every 10 mm. Fig. 5 shows beam reconstruction for: (a) off-centre wire, (b) off-centre bead, (c) centred wire, and (d) centred bead. In each case the beam is shown at axial positions $z_I = 0$ mm, 30 mm, 60 mm and 90 mm from the obstruction. Full reconstruction is found at $z = 70$ mm for the bead, and at $z = 27$ mm for the wire.

Our approach to calculating the BLB shadow after the obstruction is based on the conical wave approach. By considering the projection of the obstruction in space which results from the two travelling conical waves which produce the BLBs [30] we are able to predict the movement of the shadow region of the obstructed area with beam propagation. The approach of projecting the obstruction boundaries rather than the field itself results in the fast and accurate prediction of the field after an obstruction. We successfully predict the reconstruction properties of a BLB after obstructions in both the central region of beam and off-centre by calculating the boundaries of the various projected regions (see Fig. 5). The projection results in the creation of two zones defined by a single conical wave, with the boundaries of these zones moving farther apart at a rate of $\delta = 2z\ \tan[\theta(z)]$, where $\theta(z)$ is the cone angle at the obstruction position (see Table 1) and z is the longitudinal position of obstruction.

For each position z_I of each experiment the shadow pattern predicted by the simulation is shown as an inset. It is clear that the shadow pattern is characteristic of the shape of obstruction, as well as

the position of the obstruction in the beam. Fig. 5 reveals good agreement between the theory and the experimental results.

In our third experiment we investigated the dependence of reconstruction distance z_r on the distance z of the obstruction from the initial plane at the SLM. A wire with diameter 0.7 mm was placed off-centre in the same BLB as generated previously (i.e. $n = 1, m = 2, w = 1.7$ mm, $a = 0.05$ and $r_I = 2$ mm), first (a) at $z = 248$ mm, and then (b) at $z = 748$ mm. A camera captured the beam at a distance z_I after the obstruction.

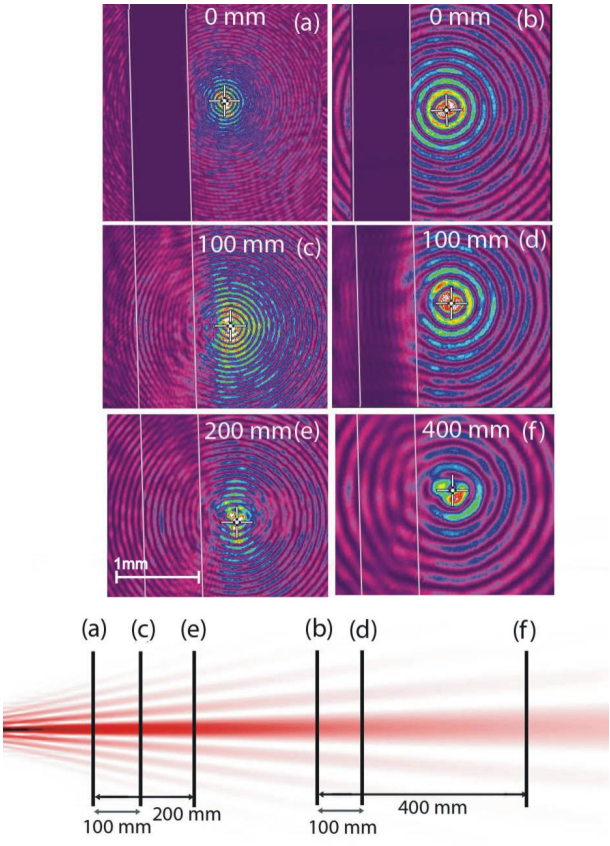

Figure 6. The self-reconstruction of the same beam with a wire obstruction placed off-centre at (a) 248 mm, and (b) 748 mm. (c) shows that the beam is partially reconstructed 100 mm after (a), contrasted with (d) which shows very little reconstruction 100 mm after (b). (e) shows complete reconstruction of the obscured area at 200 mm after (a), but (f) shows that complete reconstruction is only evident at 400 mm after (b).

Referring to Fig. 6, we observed that in both cases reconstruction is incomplete after 100 mm, but for (a) reconstruction is complete at 200 mm, whereas for (b) reconstruction was only complete after 400 mm.

4. Conclusion

Here we demonstrate the self-healing property of Bessel-like beams. We outline theoretically and confirm experimentally that the shadow region is dependent on where the obstruction is placed in the field, with the self-healing distance increasing with distance from the source plane.

Appendix

From the stationary phase approximation we can find the mapping of rays from the initial plane r_i to some screen plane r_s a distance z away, given by

$$anr_i^{n-1} + bmr_i^{m-1} + \frac{r_i}{z} - \frac{r_s}{z} = 0. \tag{8}$$

Now consider the case where the central part of the beam is obscured by an obstruction with half-width r_0 which self-reconstructs after distance z_r. We need to solve the following two simultaneous equations for z_r:

$$anr_i^{n-1} + bmr_i^{m-1} + \frac{r_i}{z} - \frac{r_0}{z} = 0 \tag{9a}$$

$$anr_i^{n-1} + bmr_i^{m-1} + \frac{r_i}{z + z_r} = 0 \tag{9b}$$

which describe the propagation of ray AC (see Fig. 1) from the initial plane r_i to (Eq. 9a) the obstruction plane at z, and to (Eq. 9b) the reconstruction plane at distance z_r beyond z where AC intersects with the optical axis OC. These equations can equally be written in terms of the cone angle at some distance z:

$$\theta + an(r_I)^{n-m}(z\theta)^{m-1} + an[-r_I^{n-m}(-r_I + 2z\theta)^{m-1} + (-r_I + 2z\theta)^{n-1}] - an(z\theta)^{n-1} = 0. \tag{10}$$

Once this is solved for θ (which will be a function of z) the reconstruction distance can be found from trigonometric arguments.

References

[1] Durnin J, 1987 *J. Opt. Soc. Am. B* **4(4)**, 651–654
[2] Durnin J, Miceli J J Jr. and Eberly J H, 1987 *Phys. Rev. Lett.* **58(15)**, 1499–1501
[3] McGloin D and Dholakia K, 2005 *Contemp. Phys.* **46(1)**, 15–28
[4] Mazilu M, Stevenson D J, Gunn-Moore F and Dholakia K, 2010 *Laser Photon. Rev.* **4(4)**, 529–547
[5] Dudley A, Lavery M, Padgett M J and Forbes A, 2013 *Opt. Photonics News* **24(6)**, 22–29
[6] Vyas S, Kozawa Y, Sato S, 2011 *JOSA A* **28(5)** 837
[7] McLaren M, Mhlanga T, Padgett M J, Roux F S, Forbes A, 2014 *Nat. Commun.* **5** 1–8
[8] MacDonald R P, Boothroyd S A, Okamoto T, Chrostowski J, Syrett B A, 1996 *Opt. Commun.* **122(4)** 169-177
[9] Bouchal Z, Wagner J, Chlup M, 1998 *Opt. Commun.* **151** 207–211
[10] Bouchal Z, 2002 *Opt. Commun.* **210(3)** 155-164

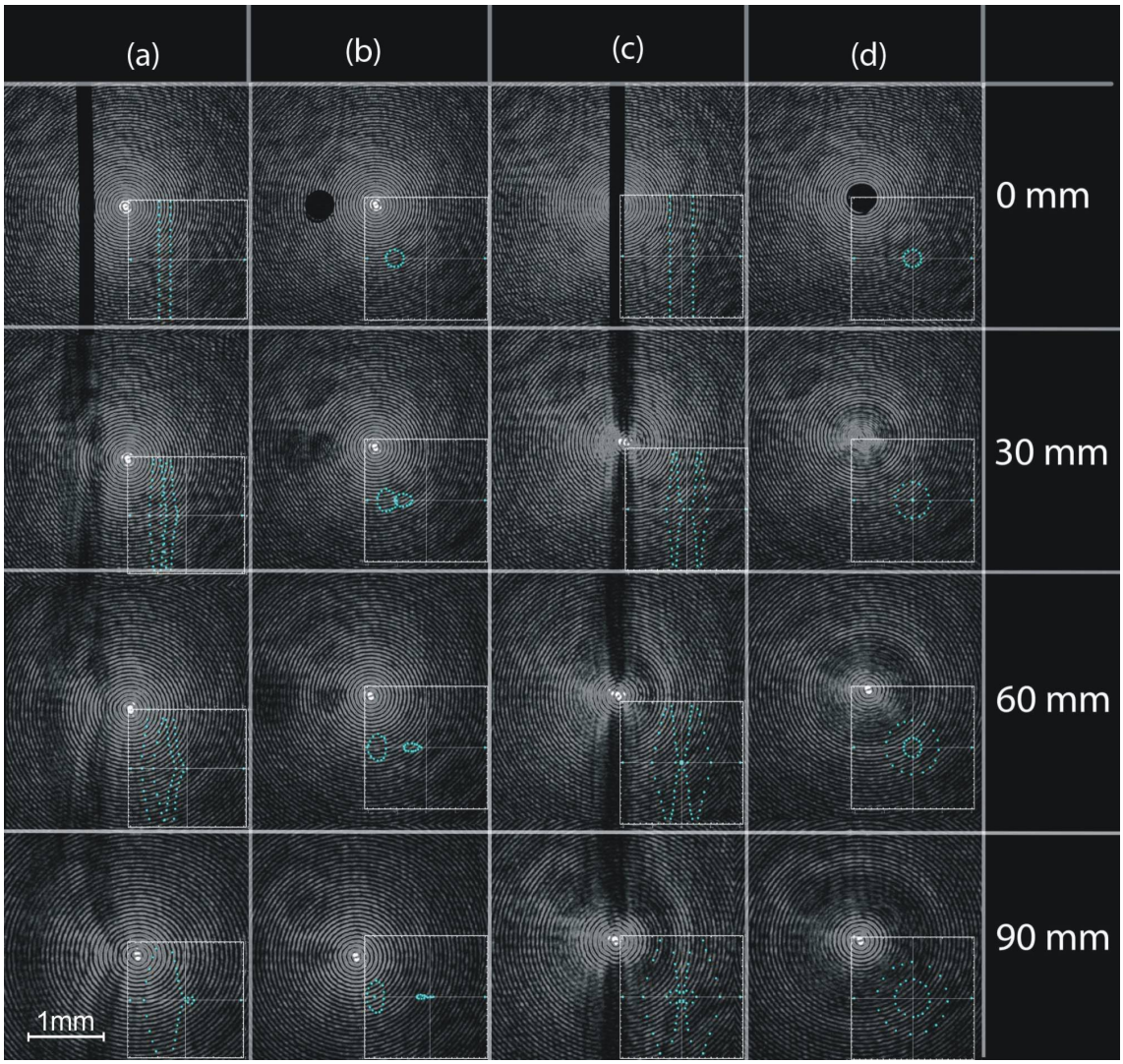

Figure 5. Beams shown at increasing distances z_I from the obstruction of four reconstruction experiments: (a) off-centre wire, (b) off-centre bead, (c) centred wire, and (d) centred bead. In each case the calculated shadow pattern is shown (inset) for $n = 1, m = 2, w = 1.7$ mm, and $a = 0.05$ and $r_I = 2$ mm.

[11] Broky J, Siviloglou G A, Dogariu A, Christodoulides D N, 2008 *Opt. Express* **16(17)** 12880-12891
[12] Arrizon V, Aguirre-Olivas D, Mellado-Villaseor G, Chavez-Cerda S, 2015 *arXiv:1503.03125 [physics]*
[13] Rop R, Litvin I A, Forbes A, 2012 *J. Opt.* **14(3)** 035702
[14] Hermosa N, Rosales-Guzmn C, Torres J P, 2013 *Opt. Lett.* **38(3)** 383–385
[15] Litvin I A, Burger L, Forbes A, 2013 *Opt. Lett.* **38(17)** 3363-3365.
[16] Ahmed N, Lavery M P J, Huang H, Xie G, Ren Y, Yan Y, Willner, A E, 2014 *2014 ECOC* 1-3
[17] Cotterell M I, Mason B J, Carruthers A E, Walker J S, Orr-Ewing A J and Reid J P, 2014 *Phys. Chem. Chem. Phys.* **16(5)** 2118–2128
[18] Eckerskorn N, Li L, Kirian R A, Kpper J, DePonte D P, Krolikowski W, Lee W M, Chapman H N, Rode A V, 2013 *Opt. Express* **21(25)** 30492
[19] Fahrbach F O, Simon P, Rohrbach A, 2010 *Nat. Photonics* **4(11)** 780-785
[20] Fahrbach F O, Rohrbach A, 2012 *Nat. Commun.* **3** 632
[21] Purnapatra S B, Bera S, Mondal P P, 2012 *Sci. Rep.* **2** 692
[22] Garces-Chavez V, McGloin D, Melville H, Sibbett W, Dholakia K, 2002 *Nature* **419(6903)** 145-147
[23] Ruffner D B and Grier D G, 2012 *Phys. Rev. Lett.* **109(16)**, 163903
[24] Cizmar T, Brzobohaty O, Dholakia K and Zemanek P, 2011 *Laser Phys. Lett.* **8(1)** 50
[25] Sokolovskii G S, Dudelev V V, Losev S N, Soboleva K K, Deryagin A G, Kuchinskii V I, Sibbett, W, Rafailov E U, 2014 *J. Phys.: Conf. Ser.* **572(1)** 012039
[26] Aiello A, Agarwal G S, 2014 *Opt. Lett.* **39(24)**, 6819–6822
[27] Aiello A, Agarwal G S, 2015 *arXiv preprint arXiv:1501.05722*
[28] Aruga T, 1997 *Appl. Opt.* **36(16)** 3762–3768
[29] Litvin I A, Mhlanga T, Forbes A, 2015 *Opt. Express* **23(6)** 7312–7319
[30] Litvin I A, McLaren M G and Forbes A, 2009 *Opt. Commun.* **282(6)**, 1078–1082
[31] Parigger C, Tang Y, Plemmons D H and Lewis J W, 1997 *Appl. Opt.* **36(31)**, 8214–8221